Journal of Vegetation Science **23** (2012) 187–197

Reconstructing savanna tree cover from pollen, phytoliths and stable carbon isotopes

Julie Aleman, Bérangère Leys, Roger Apema, Ilham Bentaleb, Marc A., Dubois, Barthélémy Lamba, Judicaël Lebamba, Céline Martin, Alfred Ngomanda, Loïc Truc, Jean-Michel Yangakola, Charly Favier & Laurent Bremond

Keywords
$\delta^{13}C$; Africa; LAI; Phytoliths; Pollen; Savanna; Woody cover

Nomenclature
Boulvert, Y. (1986)

Received 9 February 2011
Accepted 16 July 2011
Co-ordinating Editor: Kerry Woods

Aleman, J. (corresponding author, julie.aleman@univ-montp2.fr): Centre for Bio-Archeology and Ecology (CBAE; Université Montpellier 2, CNRS), Paleoenvironments and Chronoecology (PALECO; Ecole Pratique des Hautes Etudes) and UR B&SEF (CIRAD), Montpellier, France
Leys, B. (berangere.leys@univ-montp2.fr) & **Bremond, L.** (laurent.bremond@univ-montp2.fr): Centre for Bio-Archeology and Ecology (CBAE; Université Montpellier 2, CNRS) and Paleoenvironments and Chronoecology (PALECO; Ecole Pratique des Hautes Etudes), Montpellier, France
Apema, R. (apema_roger@yahoo.fr), **Lamba, B.** (lamba_barth@yahoo.fr) & **Yangakola, J.-M.** (yangakola@yahoo.fr): Laboratoire de Biologie Végétale et Fongique, Université de Bangui, Bangui, Central African Republic
Bentaleb, I. (Ilham.Bentaleb@univ-montp2.fr)
Martin, C. (celine.martin@univ-montp2.fr)
Truc, L. (loic.truc@univ-montp2.fr) & **Fravier, C.** (charly.favier@univ-montp2.fr): Institut des Sciences de l'Evolution de Montpellier, Université Montpellier 2, CNRS, IRD, France

Abstract

Aim: To calibrate a model of the relationship between bio-proxies (pollen, phytoliths and $\delta^{13}C$ of soil organic matter) and woody cover, measured as the leaf area index (LAI). This relationship, applied in palaeosequences, enables reconstruction of past savanna tree cover.

Location: The samples are from tropical Africa. Modern soil samples are from the Central African Republic and past samples are from sediments of lakes in Senegal and Congo.

Methods: We analysed the pollen and phytolith content and stable carbon isotope values of 17 soil samples taken from three short transects in the Central African Republic; LAI was measured on the same transects. The indices used were the *AP*/*NAP* ratio of arboreal (*AP*) to non-arboreal (*NAP*) pollen, the *D*/*P* ratio of ligneous dicotyledons (*D*) to Poaceae (*P*) phytoliths, and the $\delta^{13}C$ of soil organic matter, i.e. the $^{13}C/^{12}C$ ratio.

Results: A multi-proxy model was calibrated. The best model included only a combination of pollen and phytolith as proxies, excluding organic matter $\delta^{13}C$ because of its long mean residence time in the soil. The model was then applied to two palaeosequences in Africa, and a time series of relative LAI changes was obtained, providing new information about vegetation changes.

Conclusion: This model can be applied in palaeosequences to reconstruct relative time series of LAI in African savannas and can help interpret vegetation changes quantitatively. This approach is complementary to the description of pollen and phytolith assemblages.

Dubois, M.A. (mad@cea.fr): Service de physique de l'état condensé, CEA, CNRS, Saclay, France
Lebamba, J. (lebamba@cerege.fr): Centre Européen de Recherche et d'Enseignement en Géosciences de l'Environnement (CEREGE), CNRS, Université Paul Cézanne, Aix-en-Provence, France
Ngomanda, A. (ngomanda@yahoo.fr): Institut de Recherche en Ecologie Tropicale, CENAREST, Libreville, Gabon

Introduction

Savannas are one of the most important biomes in Africa. Trees and grasses co-dominate and, aside from floristic composition, the varying density of the woody element is the main characteristic used to define different types of savannas. The factors that determine the relative proportions of trees and grasses across the different types of savanna are still debated (Scholes & Archer 1997; Sankaran et al. 2005). Because savannas (especially African savannas) are expected to be among the most sensitive ecosystems to future climate changes (Sala et al. 2000; Bond et al. 2003), as they were during the Holocene (Vincens et al. 1999), we need a better understanding of these factors. Understanding past interactions between tree cover and these determining factors is of major interest. The first step is

Doi: 10.1111/j.1654-1103.2011.01335.x

reconstructing past savanna tree cover. Although the woody cover of present savannas can be measured directly, this is obviously not the case for palaeo-ecological studies, where bio-proxies are needed to provide information about past vegetation. Three bio-proxies are frequently used:

1. In pollen analysis, the ratio of arboreal (*AP*) to non-arboreal (*NAP*) pollen is commonly used to provide qualitative information about the tree cover to distinguish wooded from more open ecosystems (Liu et al. 1999; Vincens et al. 2000). A few authors have used this ratio to quantitatively estimate tree cover; for North American vegetation, see Williams (2003), for France, see Favre et al. (2008) and for South Africa, see Gillson & Duffin (2007).
2. The ratio of woody dicotyledons (*D*) to Poaceae (*P*) phytoliths was recently used to qualitatively describe vegetation types in tropical environments (Alexandre et al. 1997; Barboni et al. 1999, 2007) and Bremond et al. (2005a) calibrated this ratio against LAI.
3. ^{13}C abundance ($\delta^{13}C$) in soil organic matter in tropical environments is assumed to reflect the balance between plants with C_3 and C_4 photosynthetic pathways, with different proportions resulting in different $^{13}C/^{12}C$ ratios. Nearly all trees possess the C_3 photosynthetic pathway, and about 50% of grasses use the C_4 photosynthetic pathway (Kelly et al. 1998). In tropical environments, most savanna grasses possess the C_4 photosynthetic pathway. Thus, the $\delta^{13}C$ of soil can be used as an indicator of the differential abundance of trees and grasses and is widely used for the qualitative description of forest–savanna dynamics and grassland–woodland boundaries. This proxy has already been calibrated quantitatively in savannas against plant biomass (Gillson et al. 2004) to reconstruct past vegetation.

Each of these proxies is used to provide information about the tree–grass balance in the vegetation, but few studies have quantitatively calibrated bio-proxies against a measure of tree density (Gillson et al. 2004; Bremond et al. 2005a; Gillson & Duffin 2007; Favre et al. 2008), and up to now, no study has combined them. The aim of the present study was to calibrate a model using the three bio-proxies and leaf area index (LAI) in an African savanna. The application of this model in palaeosequences could improve the accuracy of vegetation reconstruction. We selected three experimental transects in savannas and forest–savanna transition areas in the Central African Republic. LAI was measured and surface soil samples collected for proxy analyses. Single and multiple linear regressions between LAI and the proxies were tested to calibrate the relationship. Using this calibration, we analysed two palaeosequences from Lake Guiers in Senegal and Lake Sinnda in Congo, for which pollen and phytoliths were available (Lézine 1988; Alexandre et al. 1997; Vincens et al. 1998).

Methods

Study sites for calibration

Field sites are located in the Ombella-Mpoko and Lobaye provinces of the Central African Republic (Fig. 1), a region where the rain forest progressively gives way to savannas, on ferralsols under a typical tropical climate consisting of an alternation of a dry season from Nov to Feb followed by a 8-mo long wet season, with about 1500 mm annual precipitation (Bangui weather station, FAOCLIM).

The two sampled sites are about 30 km north and south of the main forest edge. The Boali site (4°44′N, 18°02′E) supports wooded grasslands interspersed with gallery forests. The Kapou site (4°13′N, 18°18′E) is in a region of savannas included in the seasonal semi-evergreen forest domain. At both sites, savanna grass cover is about 2-m tall, with *Imperata cylindrica* as the dominant grass species, associated with typical fire-resistant trees including *Albizia zygia*, *Annona senegalensis*, *Anogeissus leiocarpa*, *Bridelia ferruginea*, *Burkea africana*, *Crossopteryx febrifuga*, *Daniellia oliveri*, *Hymenocardia acida*, *Parinari curatellifolia*, *Nauclea latifolia*, *Piliostigma thonningii*, *Terminalia glaucescens*, *Vitex doniana* and *Vitex madiensis* (Boulvert 1986).

Three transects were studied: (1) T1: 120-m long transect at Boali, through a savanna with *Anogeissus leiocarpa, Parinari curatellifolia, Annona senegalensis, Vitex ferruginea* and *Daniellia oliveri* as the main tree species; (2) T2: 120-m long transect at Boali through savanna and a clump of forest regrowth with *Manilkara multinervi* and *Craterispermum cerinanthum*; and (3) T3: 140-m long transect at Kapou across the boundary between a savanna with *Terminalia glaucescens*, *Albizia zygia* and *Vitex doniana* and a semi-deciduous forest with *Celtis zenkeri* as the main tree species.

Field sampling design

We used the leaf area index (LAI) of the tree canopy as a vegetation structure indicator (Favier et al. 2004; Scholes et al. 2004). LAI is the cumulative leaf area above the ground per unit of soil surface expressed in square meters of leaves per square meter of ground. LAI is an important property of plant communities because it is strongly correlated to the photosynthetic and water exchange characteristics of the canopy (Simioni et al. 2003). The LAI measurements were made using the LAI-L described in Cournac et al. (2002). The principle of this method, which is fast and easy to implement, is to measure the light transmitted (*I*) by the tree cover with a light-dependent resistor behind an off-the-shelf fish-eye lens (spy-hole optic). The Beer–Lambert law relates the transmitted light to the incident light I_0:

Doi: 10.1111/j.1654-1103.2011.01335.x

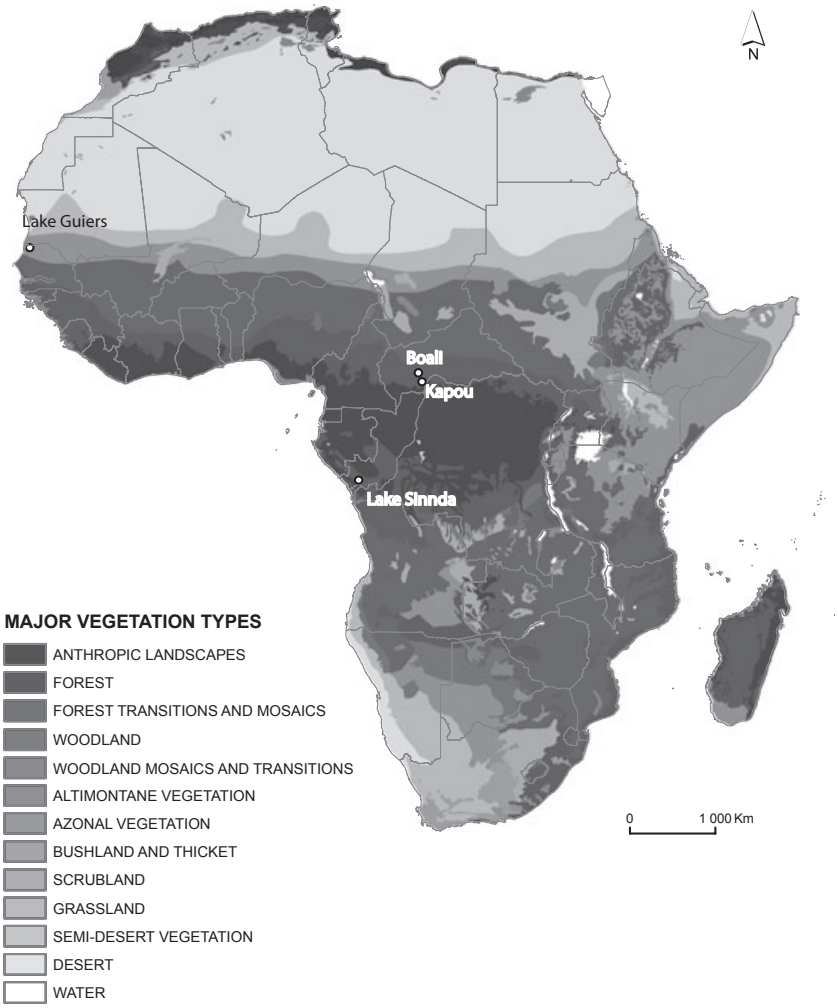

Fig. 1. Map of African major vegetation types [from White (1983)]: calibration transects (Boali and Kapou, Central African Republic) and application zones (Lake Guiers, Senegal; Lake Sinnda, Congo).

$$I = I_0 \times e^{-k.LAI}$$

I_0 is evaluated and corrected for cloud cover as explained in detail in Cournac et al. (2002). The attenuation factor k is taken equal to 0.88 (Wirth et al. 2001), as discussed in Emmons & Dubois (2003). Light readings were taken between 11:00 and 13:00 h to ensure near-vertical insolation, at 1-m intervals for all transects. The light sensor was held at 2-m height and only foliage above this level influenced the readings.

A total of 17 homogenized surface soil samples was collected. Each transect was divided into 20-m sections, on which surface soil samples were collected within a distance of 10 m from the transect, following the guidelines described in Wright (1967) and commonly used in Africa (e.g. Jolly et al. 1996; Vincens et al. 2000; Lebamba et al. 2009): a sample is composed of 20 subsamples randomly collected over the plot, after removing litter from the soil surface, and the homogenized. All trees >10 cm DBH (diameter at breast height) were surveyed in the 20-m-wide strip transect, to calculate stem density per vegetation type (savanna, pioneer and forest trees; expressed in stems.ha^{-1}).

Pollen analyses (*AP/NAP*)

Pollen concentrates were prepared from each surface soil sample following standard methods (Faegri & Iversen 1975). Then pollen grains and spores were counted and identified with the help of the reference collection of modern specimens from tropical Africa at the ISE-M laboratory (Montpellier), pictures on the African Pollen Database website (http://medias3.mediasfrance.org/apd/) and published pollen atlases related to Central Africa (Van Campo 1957; Association des Polynologues de League France

Doi: 10.1111/j.1654-1103.2011.01335.x

1974). Each pollen taxon was attributed to arboreal (*AP*) or non-arboreal (*NAP*) following Vincens et al. (2007b), and expressed as the *AP/NAP* ratio.

$\delta^{13}C$ isotopic composition

Carbon isotope analyses were performed on bulk organic matter containing about 100 mg (dry weight) of soil samples. The samples were dried at 40 °C. Particles not passing a 2-mm screen were removed, while soil passing the 2-mm screen was ground by hand using a mortar pillar to pass through a 200-μm mesh. CO_2 gas for carbon isotope analysis was obtained by combustion of the samples at 1020 °C using a Euro Vector 3000 elemental analyser coupled to a VG Optima mass spectrometer.

Carbon isotopic composition ($\delta^{13}C$) is expressed in per mil with respect to the international V-PDB (Vienna-Pee-Dee-Belemnite) standard:

$$\delta^{13}C = \left(\frac{R_{sample}}{R_{standard}} - 1\right) \times 1000, \text{where } R = {}^{13}\text{C}/{}^{12}\text{C}$$

The standard deviation of replicate runs is ca. 0.2.

Phytolith analyses (*D/P*)

Phytoliths were extracted with the protocol described in Bremond et al. (2005a). The recovered fraction, including primarily opal phytoliths, was mounted on microscope slides in immersion oil and counted at 600× magnification. More than 250 phytoliths per sample, with taxonomic significance and greater than 5-μm diameter (minimum size for determination), were counted and classified according to the International Code for Phytolith Nomenclature (Madella et al. 2005). Phytoliths were defined as typical of dicotyledons [rough and smooth spherical; *D*; (Bremond et al. 2005a)] or as typical of Poaceae types (grass silica short cells: dumbbell, cross, saddle, conical, polylobate; *P*). Fan-shaped, point-shaped and elongate types were not included in calculation of *P* because their production is dependent on environmental conditions (Bremond et al. 2005b). The data are expressed as *D/P*, ratio of *D* over *P* phytolith number.

Statistical analyses: error estimations

Quantifying the various sources of error from pollen and phytolith analysis remains difficult and uncertain. The first error may come from pollen and phytolith rains over the soil and the proportion remaining in litter. Other errors may then come from the sampling method, the treatment, and finally from counting. Thus, we preferred to compute a theoretical statistical confidence interval that includes all error types.

Let n_D be the number of *D* phytoliths, n_P be the number of *P* phytoliths and $n = n_D + n_P$, the $1-\alpha$ confidence interval of the *D/P* index is when *n* is large, $[I_{\alpha-}; I_{\alpha+}]$, with:

$$I_{\alpha\pm} = \frac{1 + \frac{n_D}{n_P}}{1 \pm \frac{z_{1-\alpha/2}}{\sqrt{n}}\sqrt{\frac{n_D}{n_P}}} - 1$$

where $z_{1-\alpha/2}$ is the $1-\alpha/2$ percentile of a standard normal distribution (see Appendix S1 for demonstration, Wald (1940)). This formula matches bootstrap estimates found by Stromberg (2009) for *n* up to 2000 with 10 000 replicates.

The same reasoning is used for pollen counts, with n_{AP} the number of arboreal pollen, n_{NAP} the number of non-arboreal pollen and $n = n_{AP} + n_{NAP}$. The $1-\alpha$ confidence interval of the *AP/NAP* index is when *n* is large, $[I_{\alpha-}; I_{\alpha+}]$, with:

$$I_{\alpha\pm} = \frac{1 + \frac{n_{AP}}{n_{NAP}}}{1 \pm \frac{z_{1-\alpha/2}}{\sqrt{n}}\sqrt{\frac{n_{AP}}{n_{NAP}}}} - 1$$

Univariate and multivariate analyses

Linear regressions were performed between mean stand LAI as the response variable and different transformation of *D/P*, *AP/NAP* and $\delta^{13}C$ as explanatory variables. We tested different transformation of the proxies to determine which, in single-factor regressions, best relates to LAI; in addition to untransformed variables, we used exponential, decimal and natural logarithm forms. Spearman's correlation coefficients (*R*) were calculated between the fitted LAI values estimated by the regression models and the measured values, and were used to confirm the validity of the calibration in association with a correlation test (*P*-value computation). We used a step-wise algorithm in R 2.13.0 software (R Core Development Team, Vienna, AT), the 'step' function, which selects from individual variables in a multiple statistical model using the Akaike information criterion (AIC).

Application to palaeosequences

We consider the upper parts of two palaeosequences from lake cores from which both pollen and phytoliths were previously counted: the core S2 (from the top to 360 cm) from Lake Guiers (16°15′N, 15°50′W), which is now surrounded by a Sahelian sparse shrub savanna (Lézine 1988; Lézine & Casanova 1989; Alexandre et al. 1997) and the core SN2 (from the top to 71 cm) from Lake Sinnda (3° 50′S, 12°48′E), now surrounded by a wooded savanna

Doi: 10.1111/j.1654-1103.2011.01335.x

(Alexandre et al. 1997; Vincens et al. 1998). In these palaeosequences, pollen types indicated in the publications as typical of aquatic and swampy environments were excluded from the total of arboreal and non-arboreal pollens: e.g. *Nymphea,* Cyperaceae, *Typha* and *Rhizophora.*

Each published ^{14}C date along the sequences was calibrated in years Before Present (hereafter cal. yr BP) using the CALIB program (Stuiver & Reimer 1993) version 6.0.1. An age–depth model was then calculated with the MCAgeDepth program (Higuera et al. 2009).

Results

Bio-proxies and LAI along the plots

Changes in vegetation structure along the three transects, represented by LAI, co-vary with *D/P*, *AP/NAP* and $\delta^{13}C$ (Fig. 2). On transect T2, the forest clump is represented by an increase of LAI and appearance of pioneer trees. The *D/P* has higher values than in savanna, as well as $\delta^{13}C$, except for its last value, which is similar to those of savanna. In contrast, *AP/NAP* values do not differ between savannas and forest clumps. The T3 transect transition from savanna to forest is characterized by increasing LAI values from < 2 in savanna to > 4 in the forest front. *D/P* and *AP/NAP* increase at the transition, whereas $\delta^{13}C$ decreases. Nevertheless, the $\delta^{13}C$ values in a portion of the savanna (60–100 m) are typical of closed vegetation, whereas LAI values are still those of savanna.

A model for reconstructing vegetation structure from bio-proxies

Each bio-proxy is plotted against LAI (Fig. 3a–c). Phytolith (*D/P*) and pollen (*AP/NAP*) indices (transformed as $\ln(\frac{D}{P}+1)$ and $\ln(\frac{AP}{NAP}+1)$) were strongly related to LAI (respectively $R = 0.855$; $n = 17$; $P < 0.001$, Fig. 3d; and $R = 0.931$; $n = 17$; $P < 0.001$, Fig. 3e). Three zones are visible on the $\delta^{13}C$ vs LAI plot (Fig 3c): an area of closed-canopy woody vegetation ($\delta^{13}C < -25$), a transition area, and an area of open vegetation ($\delta^{13}C > -20$). The exponential transformation $e^{-\delta 13C}$ has the best correlation coefficient ($R = 0.915$; $n = 17$; $P < 0.001$, Fig. 3f). These results are summarized in Table 1.

When performing multiple linear regressions of LAI against transformed proxies, $\delta^{13}C$ does not appear to be a significant explanatory variable (*P*-value > 0.5, Table 2), and the final relationship only contains *D/P* and *AP/NAP* as explanatory variables:

$$\mathrm{LAI} = 2.216 \times \ln\left(\frac{D}{P}+1\right) + 0.885 \times \ln\left(\frac{AP}{NAP}+1\right) \quad (1)$$

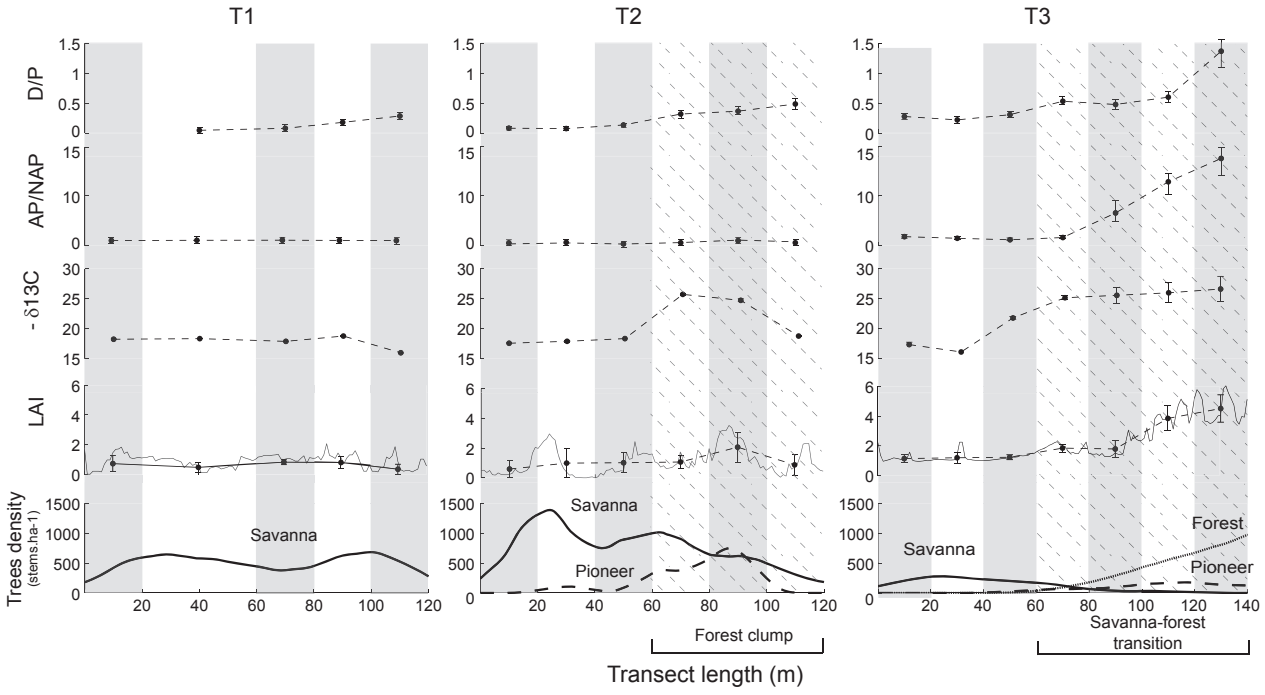

Fig. 2. Vegetation structure, as indicated by LAI (leaf area index) and tree density (number of stems per hectare), and bio-proxies values along three transects: through a savanna (T1), a savanna with forest clump (T2), and a savanna-forest transition (T3) in Central African Republic.

Doi: 10.1111/j.1654-1103.2011.01335.x

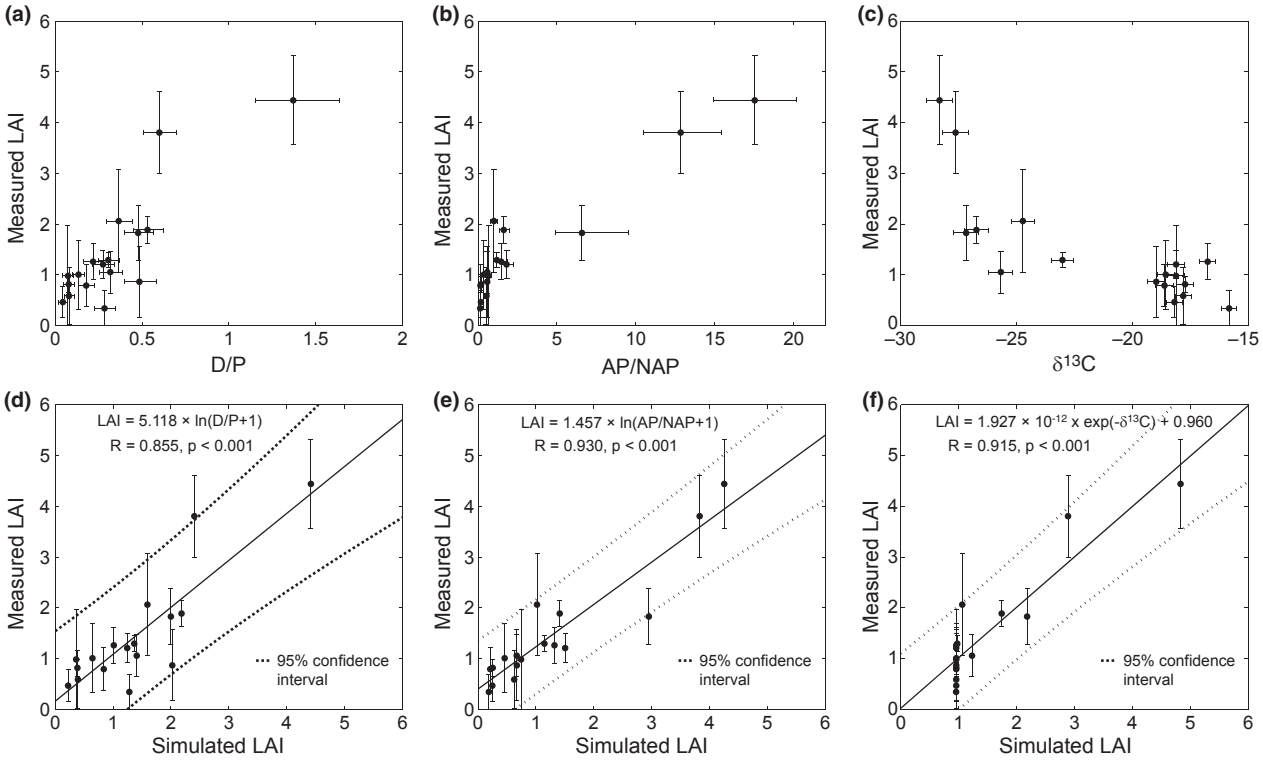

Fig. 3. Plots of bio-proxies against LAI measured above 2 m (**a**–**c**) and corresponding simple linear regression (**d**–**f**). The coefficients of each regression are presented in Table 1.

Table 1. Coefficients and associated characteristics for each proxy in simple linear regressions.

Proxy	Regression equation	95% Confidence Limits		*R*	*P*-value
		Slope	Intersect		
D/P	$LAI = 5.118 \times \ln(\frac{D}{P}+1)$	± 0.897	–	0.855	<0.001
AP/NAP	$LAI = 1.457 \times \ln(\frac{AP}{NAP}+1)$	± 0.213	–	0.931	<0.001
δ^{13C}	$LAI - 1.927 \times 10^{-12} \times e^{-\delta 13C} + 0.956$	± 0.447 × 10^{-12}	± 0.251	0.915	<0.001

Table 2. Regression coefficients values, errors and *P*-values for each proxy in multiple regressions (a- with the three proxies, b- with only *D/P* and *AP/NAP*).

Proxy	Coefficient	SE	*P*-value
a.			
$\ln(\frac{D}{P}+1)$	2.226	± 0.777	<0.001
$\ln(\frac{AP}{NAP}+1)$	0.918	± 0.260	<0.001
$e^{-\delta 13C}$	-8.601×10^{-14}	± 3.697×10^{-13}	0.82
b.			
$\ln(\frac{D}{P}+1)$	2.216	±0.750	0.010
$\ln(\frac{AP}{NAP}+1)$	0.885	±0.210	<0.001

As expected, simulated and measured LAI values are tightly correlated (Fig. 4, $R = 0.942$, $n = 17$, $P < 0.001$).

Application to palaeosequences: an illustration

We hypothesize that, as in our calibration study, $\ln(\frac{D}{P}+1)$ and $\ln(\frac{AP}{NAP}+1)$ are surrogates for savanna tree LAI. Due to differences in catchment areas and in transportation and deposition processes, reconstructing LAI requires calibration of the regression coefficients for each site. Considering that the regression coefficients of the multiple model are significantly close to half the coefficients of the simple models, it is therefore possible to express LAI up to a multiplicative factor:

$$\mathrm{LAI} \propto \left[\gamma \ln\left(\frac{D}{P}+1\right) + \ln\left(\frac{AP}{NAP}+1\right)\right],$$

where γ is the slope of the linear regression through the origin of $\ln(\frac{AP}{NAP}+1)$ on $\ln(\frac{D}{P}+1)$ on (see Appendix S2 for details).

Time series of LAI are normalized to 1 at the most recent sample.

In the Lake Guiers core, using *D/P* and *AP/NAP*, three zones of reconstructed LAI are distinguishable (Fig. 5a).

Doi: 10.1111/j.1654-1103.2011.01335.x

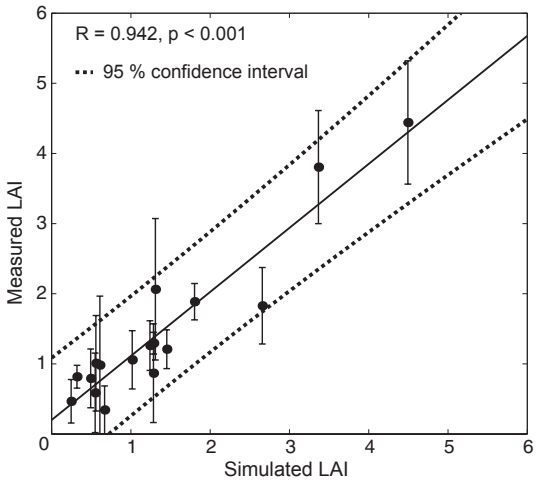

Fig. 4. Model plot of simulated vs measured values of LAI. Simulated LAI values come from multiple regression using *D/P* and *AP/NAP* (Table 2b).

From 5200 to 2000 cal. yr BP, LAI values were more than 25 times the present vegetation and probably correspond to a wooded savanna. There are low percentages of aquatic taxa (*Nymphea)* and swampy taxa (Cyperaceae and *Typha*) but mangrove (*Rhizophora*) pollen is present. The arboreal pollen assemblage is essentially composed of Sudanian and Sudano-Guinean taxa (Combretaceae, *Celtis integrifolia, Acacia*-type and *Cassia*-type). The percentages of grass pollen are very low. Then, a transition zone from 2000 to 1300 cal. yr BP corresponds to a decrease in LAI values, decreases in mangroves, and increasing percentage of swampy taxa. More diverse arboreal pollen is detected, mainly Sudanian and Sudano-Guinean elements (Lézine 1988). Finally, in the third zone (1300 cal. yr BP to present-day), the mangroves have totally disappeared, aquatic taxa are more frequent and the arboreal pollen corresponds to the modern Sahelian elements.

As described in Vincens et al. (1998), four zones can be identified in Lake Sinnda SN2. The first (1000–850 cal. yr BP) shows an increase in the reconstructed LAI by a factor of four to reach the modern vegetation cover (Fig. 5b) and corresponds to high percentages of swampy taxa (Cyperaceae and *Typha*), which indicates the start of the lake re-filling after its desiccation between 3800 and 1300 cal. yr BP. The higher proportion of *AP* taxa is represented by savanna (*Bridelia ferruginea*-type and *Lannea*-type) and forest regrowth (*Alchornea*) taxa. The second zone (850–450 cal. yr BP) shows the highest relative value of LAI, indicating the highest woody cover. This is

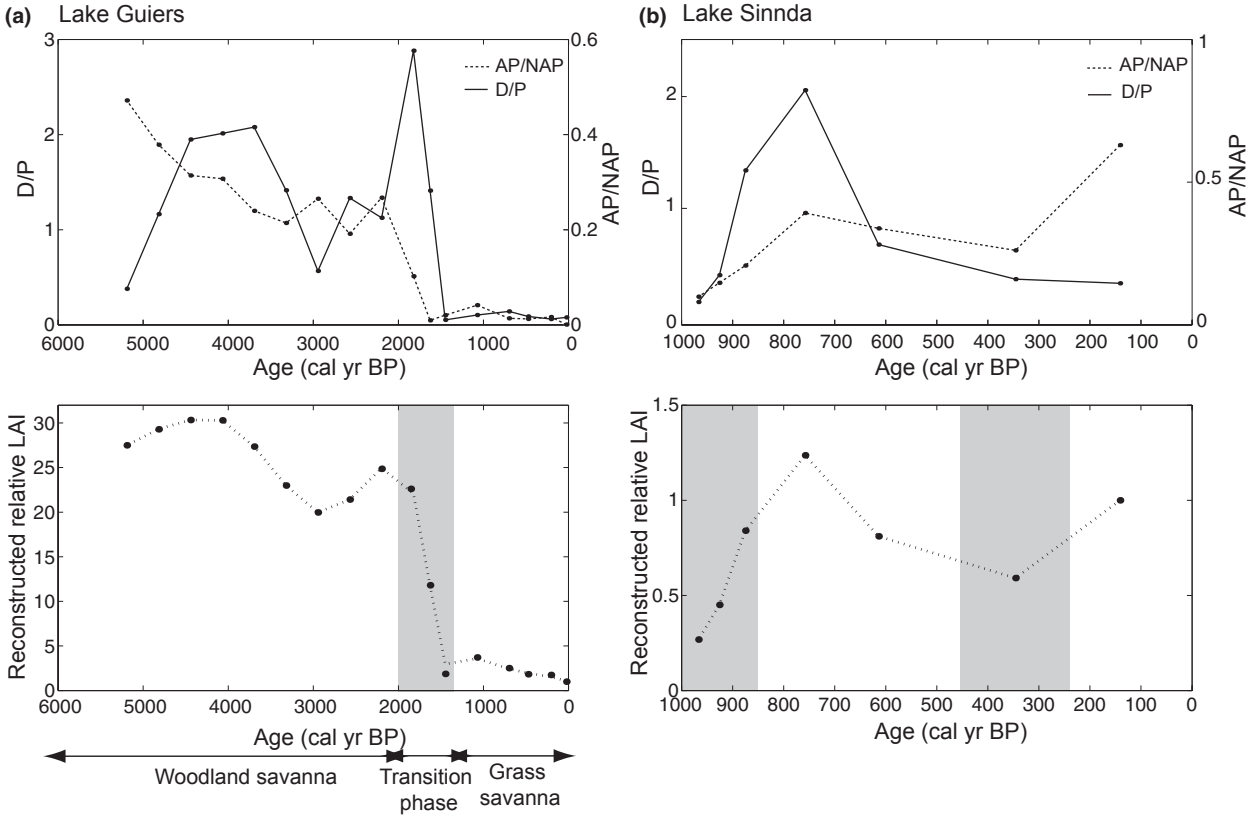

Fig. 5. Application of the model to Lake Guiers (**a**) and to Lake Sinnda (**b**), pollen and phytoliths indices (upper panels), and simulated relative LAI (lower panels).

Doi: 10.1111/j.1654-1103.2011.01335.x

correlated to an increase in rainfall, shown by a decrease in swampy taxa frequencies (rising lake water level) and an increase in frequencies of savanna trees and forest species (essentially *Alchornea*). The third zone (450–250 cal. yr BP) shows a decrease of LAI associated with an increase of swampy taxa, that can be related to a short arid phase (decrease of lake water level). Once again *Alchornea* is the major *AP* type, with few savanna taxa. The last zone (from 250 cal. yr BP) shows an increase in LAI corresponding to a more humid phase (less swampy taxa).

Discussion

The aim of the present study was to calibrate a model using three bio-proxies and the leaf area index (LAI) in an African savanna to improve the accuracy of vegetation reconstruction. Due to lack of significance of $\delta^{13}C$ as an explanatory variable, the model combines only *D/P*, the ratio of dicotyledons (*D*) over Poaceae (*P*) phytoliths, and *AP/NAP*, the ratio of arboreal (*AP*) to non-arboreal (*NAP*) pollen. This is a surprising result that will be discussed below. The application of our model to two palaeosequences provides relative LAI reconstruction that is in agreement with the pollen and phytolith assemblages described in the original studies. However, concerns about the transportation of bio-proxies and taphonomy must be considered.

Calibration of the model: temporal and spatial scales in soil samples

We calibrated our model using different proxies taken from surface soil samples. An important issue is their time resolution. Whereas LAI is an instantaneous measure of the state of the vegetation, the bio-proxies incorporate vegetation states over a period that corresponds to their mean residence times (MRT) in the soil. In tropical soils, ^{13}C MRT is reported to depend on a variety of factors. First, C_3 organic matter decomposes faster than C_4 organic matter (Wynn & Bird 2007). Second, the difference in environmental factors under open and closed vegetation affects the mineralization rate. According to Schwartz et al. (1996) and Boutton et al. (1998), ^{13}C MRT is around 60–90 yrs in savannas vs around 30 years in forests. Although few studies have been conducted regarding the MRT of pollen and phytoliths in soils, it is nevertheless accepted that oxidizing conditions in tropical soils cause rapid destruction of pollen. Thus it is widely assumed that the pollen in surface soil samples only represents a few years of the vegetation record (Andersen 1986). In contrast, little is known about the MRT of phytoliths, but Alexandre et al. (1997) and Parker et al. (2004) reported that they are well preserved under oxidizing conditions and thus may perpetuate vegetation signals for several years. Differences in the MRT of the proxies may explain the observed discrepancies between LAI and the biological proxies along our transects. On transect T3, for example, the savanna–forest transition is well recorded by all the proxies, but a discrepancy appears between $\delta^{13}C$ values and the LAI. Indeed, the LAI for a particular 40–60-m segment points to savanna vegetation, whereas the $\delta^{13}C$ value is typical of a forest–savanna transition. This discrepancy could be the result of a recent forest recession (Schwartz et al. 1996). Unlike the $\delta^{13}C$ signal, the phytolith-based *D/P* and the pollen-based *AP/NAP* correspond well with the present savanna–forest transition. A shorter MRT for phytoliths than for ^{13}C in the soil and a higher production of phytoliths by grasses than by trees (Piperno 2006) may explain the shorter 'memory effect' of phytoliths. On transect T2, the forest clump is well recorded by the $\delta^{13}C$ except for the border (100–120 m), where the value is closer to that of an open formation, whereas *AP/NAP* and *D/P* indices record the entire clump. Again, differences in the MRT may explain this discrepancy. The clump is the result of recent forest expansion, as evidenced by pioneer trees in the botanical surveys summarized in Fig. 2 (tree densities), so the border is not recorded by $\delta^{13}C$, which needs longer times than pollen and phytoliths to indicate the new vegetation environment.

Different time resolutions of the three bio-proxies may also explain why the $\delta^{13}C$ is not a significant contributor to the calibration equation: $\delta^{13}C$ represents vegetation dynamics averaged over a longer period than pollen and phytolith proxies, while LAI is an instantaneous measure.

Another source of discrepancies between LAI and the proxies is the different spatial scales of the records. First, LAI was measured continuously along transects and samples were collected within a distance of 10 m on either side. Second, trees and shrubs that were less than 2-m tall were not included in LAI measurements but contribute to phytolith, pollen and C_3 organic matter production. Third, taphonomic processes may also play a role. The method used for LAI measurements is very sensitive to changes in tree cover over short distances (<1 m).

The $\delta^{13}C$ in soil organic matter results from the decomposition of vegetation located directly above the soil but also from the decomposition of vegetation transported short distances by run-off, wind and bioturbation. *AP/NAP* and *D/P* indices depend on the transportation of bio-proxies. Transportation of phytoliths and pollen by wind may play an important role, especially after fires, which lead to increased erosion and transport. These processes are exacerbated in open vegetation where pollen and phytolith assemblages represent a larger spatial scale than LAI. Moreover, pollen and phytoliths of grasses are known to be mainly dispersed by wind, but this is less known for trees. Nevertheless, wind dispersed and large producer

Doi: 10.1111/j.1654-1103.2011.01335.x

pollen taxa cause a bias in pollen assemblages since they are over-represented relative to dominance in the vegetation. For example, in Amazonian savannas, Jones et al. (2011) showed that the Moraceae/Urticaceae taxa completely overwhelmed savanna taxa in pollen assemblages. Only a few grains of pollen of Moraceae were found in the pollen assemblages at the three sites where our model was calibrated and applied, and the *AP* contained mainly savanna taxa.

Despite these issues, the model performs well (R = 0.942) and appears to enable reconstruction of savanna woody cover from a combination of phytolith and pollen proxies.

Model applicability to palaeosequences

Our application of the model to two palaeosequences in West Africa, where pollen and phytoliths data are available, raises questions about the transferability of a model calibrated using present-day soil surface samples and applied to lake sediment samples, as the sites are spatially and temporally distant and have different source areas of pollens and phytoliths. Nevertheless, provided care is taken with interpretation, two factors support the model's application across geographical and temporal scales. First, the method with modern analogues is widely used to reconstruct past vegetation: bio-proxy assemblages from lake sediments are compared to bio-proxy assemblages from modern soil samples. Thus, this method had already been applied in studies using pollen (Wright 1967; Vincens et al. 2007a) and phytoliths (Barboni et al. 1999). Second, despite their distance, pollen spectra at the three sites share many common pollen taxa. Moreover, we used proxies corresponding to broad categories that aggregate a range of pollen and phytolith source plants (arboreal and non-arboreal) that are assumed to be more stable than the production of one particular species (Barboni et al. 2007; Gillson & Duffin 2007).

The second concern is differences in the taphonomic processes (production, transportation, deposition and potential degradation of the bio-proxies) between soil and lake sediments. In particular, part of the pollen and the phytoliths may originate from lake shorelines whose extent is likely to vary over time and thus may not reflect the real changes in vegetation structure that occurred on *terra firme*. Typical aquatic and swampy taxa were excluded from *AP*, *NAP*, *D* and *P* indices but uncertainties remain concerning the source of some taxa, especially Poaceae and some arboreal taxa. We chose not to carry out any further selection of arboreal pollens, for example by distinguishing savanna taxa from forest taxa, as this may lead to a loss of information about forest trees becoming established in the savanna. Thus, on our calibration transects, forest clumps were present in the savanna. Moreover, such selection is not possible for phytoliths. Taken together, these approximations certainly affect the slopes between LAI and the proxies $\ln\left(\frac{AP}{NAP}+1\right)$ on $\ln\left(\frac{D}{P}+1\right)$.

When applying the model to Lake Guiers and Lake Sinnda palaeosequences, we took these limitations into account. Thus, we assumed that the coefficients of the model had changed but $\ln\left(\frac{AP}{NAP}+1\right)$ on $\ln\left(\frac{D}{P}+1\right)$ were still linearly related to LAI, as long as savanna was the major ecosystem surrounding the sites. This led to a quantification of the relative changes in the LAI of savannas surrounding the sites over time. Our reconstructions were in accordance with floristic dynamics and interpretations provided in the original studies. The precise quantification of absolute LAI evolution would require local calibration of the model on lake deposits.

Conclusion

We suggest that our model reconstructing LAI from *D/P* and *AP/NAP* can be used in various types of African savanna. Indeed, each of these proxies has already been used independently to estimate vegetation cover in different parts of Africa. The combination of two proxies (*D/P* and *AP/NAP)* improved accuracy of tree cover reconstruction and the time series of LAI obtained for both lakes is in agreement with pollen assemblages and interpretations in previous studies. The present study demonstrated the usefulness of our model in interpreting palaeosequences from lake cores. However, the sites where the model was calibrated and applied, and where samples were taken were different (soil and lake sediments, respectively), and taphonomic processes are known to differ. Few studies of the taphonomic processes of pollen and phytoliths are available and further research is needed. Research is already underway to identify the relationships between the deposition and the conservation of bio-proxies in lake sediments and the surrounding vegetation, and to estimate the impact of the shorelines on *AP/NAP* and *D/P* indices.

Acknowledgements

This study was financially supported by French Ministry of Foreign Affairs (CORUS 2 project SORCA) and the French National Research Agency (ANR, 2008-29489-62704-33) through the ErA Net BiodivERsA CoForChange project. The PhD thesis of JA is co-supported by the French CNRS and CIRAD, and directed by CF and LB. We warmly thank Arnaud Kpolita, Leticia Boyaka and Fred-Fresnel Ngapogara Dange for their contributions during the fieldwork, Laure Paradis for map design and Drs. Jack Putz and Michael Swaine for linguistic improvement on the manuscript. A special thanks to Olivier Blarquez.

References

Alexandre, A., Meunier, J.D., Lézine, A.M., Vincens, A. & Schwartz, D. 1997. Phytoliths: indicators of grassland dynamics during the late Holocene in intertropical Africa. *Palaeogeography, Palaeoclimatology, Palaeoecology* 136: 213–229.

Andersen, S. 1986. Palaeoecological studies of terrestrial soils. In: Berglund, B.E. (ed.) *Handbook of Holocene palaeoecology and palaeohydrology*. pp. 165–177. Wiley, Chichester, UK.

Association des Polynologues de League France. 1974. Pollen et spores d'Afrique tropicale. *Centre d'Etudes de Géographie Tropicale, CNRS, Talence*, FR: 282, pp. 16.

Barboni, D., Bonnefille, R., Alexandre, A. & Meunier, J. 1999. Phytoliths as paleoenvironmental indicators, west side Middle Awash Valley, Ethiopia. *Palaeogeography, Palaeoclimatology, Palaeoecology* 152: 87–100.

Barboni, D., Bremond, L. & Bonnefille, R. 2007. Comparative study of modern phytolith assemblages from inter-tropical Africa. *Palaeogeography, Palaeoclimatology, Palaeoecology* 246: 454–470.

Bond, W., Midgley, G. & Woodward, F. 2003. The importance of low atmospheric CO_2 and fire in promoting the spread of grasslands and savannas. *Global Change Biology* 9: 973–982.

Boulvert, Y. 1986. *Carte phytogéographique au 1/1 000 000, République Centrafricaine*. Notice explicative no. 104. In: Orstom, Paris, FR.

Boutton, T., Archer, S., Midwood, A., Zitzer, S. & Bol, R. 1998. ^{13}C values of soil organic carbon and their use in documenting vegetation change in a subtropical savanna ecosystem. *Geoderma* 82: 5–41.

Bremond, L., Alexandre, A., Hely, C. & Guiot, J. 2005a. A phytolith index as a proxy of tree cover density in tropical areas: Calibration with Leaf Area Index along a forest–savanna transect in southeastern Cameroon. *Global and Planetary Change* 45: 277–293.

Bremond, L., Alexandre, A., Peyron, O. & Guiot, J. 2005b. Grass water stress estimated from phytoliths in West Africa. *Journal of Biogeography* 32: 311–327.

Cournac, L., Dubois, M., Chave, J. & Riéra, B. 2002. Fast determination of light availability and leaf area index in tropical forests. *Journal of Tropical Ecology* 18: 295–302.

Emmons, L.H. & Dubois, M.A. 2003. Leaf-area index change across river–beach successional transects in south-eastern Peru. *Journal of Tropical Ecology* 19: 473–477.

Faegri, K. & Iversen, J. 1975. *Textbook of pollen analysis*. 3rd ed. Blackwell, Oxford, UK.

Favier, C., De Namur, C. & Dubois, M.A. 2004. Forest progression modes in littoral Congo, Central Atlantic Africa. *Journal of Biogeography* 31: 1445–1461.

Favre, E., Escarguel, G., Suc, J., Vidal, G. & Thévenod, L. 2008. A contribution to deciphering the meaning of AP/NAP with respect to vegetation cover. *Review of Palaeobotany and Palynology* 148: 13–35.

Gillson, L. & Duffin, K.I. 2007. Thresholds of potential concern as benchmarks in the management of African savannahs. *Philosophical Transactions of the Royal Society B-Biological Sciences* 362: 309–319.

Gillson, L., Waldron, S. & Willis, K.J. 2004. Interpretation of soil delta C-^{13} as an indicator of vegetation change in African savannas. *Journal of Vegetation Science* 15: 339–350.

Higuera, P., Brubaker, L., Anderson, P., Hu, F. & Brown, T. 2009. Vegetation mediated the impacts of postglacial climate change on fire regimes in the south-central Brooks Range, Alaska. *Ecological Monographs* 79(2): 201–219.

Jolly, D., Bonnefille, R., Burcq, S. & Roux, M. 1996. Study and statistical treatment of pollen samples from surface soil of the rain forest in Gabon (Africa). *Comptes Rendus De L'Académie Des Sciences* 322: 63–70.

Jones, H.T., Mayle, F.E., Pennington, R.T. & Killeen, T.J. 2011. Characterization of Bolivian savanna ecosystems by their modern pollen rain and implications for fossil pollen records. *Review of Palaeobotany and Palynology* 164: 223–237.

Kelly, E., Blecker, S., Yonker, C., Olson, C., Wohl, E. & Todd, L. 1998. Stable isotope composition of soil organic matter and phytoliths as paleoenvironmental indicators. *Geoderma* 82: 59–81.

Lebamba, J., Vincens, A., Jolly, D., Ngomanda, A., Schevin, P., Maley, J. & Bentaleb, I. 2009. Modern pollen rain in savanna and forest ecosystems of Gabon and Cameroon, Central Atlantic Africa. *Review of Palaeobotany and Palynology* 153: 34–45.

Lézine, A. 1988. New pollen data from the Sahel, Senegal. *Review of Palaeobotany and Palynology* 55: 141–154.

Lézine, A. & Casanova, J. 1989. Pollen and hydrological evidence for the interpretation of past climates in tropical West Africa during the Holocene. *Quaternary Science Reviews* 8: 45–55.

Liu, H., Cui, H., Pott, R. & Speier, M. 1999. The surface pollen of the woodland–steppe ecotone in southeastern Inner Mongolia, China. *Review of Palaeobotany and Palynology* 105: 237–250.

Madella, M., Alexandre, A. & Ball, T. 2005. International code for phytolith nomenclature 1.0. *Annals of Botany* 96: 253–260.

Parker, A., Eckersley, L., Smith, M., Goudie, A., Stokes, S., Ward, S., White, K. & Hodson, M. 2004. Holocene vegetation dynamics in the northeastern Rub'al-Khali desert, Arabian Peninsula: a phytolith, pollen and carbon isotope study. *Journal of Quaternary Science* 19: 665–676.

Piperno, D. 2006. *Phytoliths: a comprehensive guide for archaeologists and paleoecologists*. AltaMira Press, Lantham, MD, US.

Sala, O., Chapin, F. III, Armesto, J., Berlow, E., Bloomfield, J., Dirzo, R., Huber-Sanwald, E., Huenneke, L., Jackson, R. & Kinzig, A. 2000. Global biodiversity scenarios for the year 2100. *Science* 287: 1770.

Sankaran, M., Hanan, N.P., Scholes, R.J., Ratnam, J., Augustine, D.J., Cade, B.S., Gignoux, J., Higgins, S.I., Le Roux, X., Ludwig, F., Ardo, J., Banyikwa, F., Bronn, A., Bucini, G., Caylor, K.K., Coughenour, M.B., Diouf, A., Ekaya, W., Feral, C.J., February, E.C., Frost, P.G.H., Hiernaux, P., Hrabar, H., Metzger, K.L., Prins, H.H.T., Ringrose, S., Sea, W., Tews, J.,

Doi: 10.1111/j.1654-1103.2011.01335.x

Worden, J. & Zambatis, N. 2005. Determinants of woody cover in African savannas. *Nature* 438: 846–849.

Scholes, R. & Archer, S. 1997. Tree–grass interactions in savannas. *Annual Review of Ecology and Systematics* 28: 517–544.

Scholes, R., Frost, P. & Tian, Y. 2004. Canopy structure in savannas along a moisture gradient on Kalahari sands. *Global Change Biology* 10: 292–302.

Schwartz, D., Foresta, H., Mariotti, A., Balesdent, J., Massimba, J. & Girardin, C. 1996. Present dynamics of the savanna–forest boundary in the Congolese Mayombe: a pedological, botanical and isotopic (^{13}C and ^{14}C) study. *Oecologia* 106: 516–524.

Simioni, G., Gignoux, J. & Le Roux, X. 2003. Tree layer spatial structure can affect savanna production and water budget: results of a 3-D model. *Ecology* 84: 1879–1894.

Stromberg, C.A.E. 2009. Methodological concerns for analysis of phytolith assemblages: does count size matter? *Quaternary International* 193: 124–140.

Stuiver, M. & Reimer, P. 1993. Extended ^{14}C database and revised CALIB 3.0 ^{14}C age calibration program. *Radiocarbon* 35: 215–230.

Van Campo, M. 1957. *Palynologie africaine: I*. Institut Français d'Afrique Noire, Dakar, SN.

Vincens, A., Schwartz, D., Bertaux, J., Elenga, H. & de Namur, C. 1998. Late Holocene climatic changes in western equatorial Africa inferred from pollen from Lake Sinnda, southern Congo. *Quaternary Research* 50: 34–45.

Vincens, A., Schwartz, D., Elenga, H., Reynaud-Farrera, I., Alexandre, A., Bertaux, J., Mariotti, A., Martin, L., Meunier, J. & Nguetsop, F. 1999. Forest response to climate changes in Atlantic Equatorial Africa during the last 4000 years BP and inheritance on the modern landscapes. *Journal of Biogeography* 26: 879–885.

Vincens, A., Dubois, M.A., Guillet, B., Achoundong, G., Buchet, G., Beyala, V.K.K., de Namur, C. & Riera, B. 2000. Pollen-rain–vegetation relationships along a forest–savanna transect in southeastern Cameroon. *Review of Palaeobotany and Palynology* 110: 191–208.

Vincens, A., Garcin, Y. & Buchet, G. 2007a. Influence of rainfall seasonality on African lowland vegetation during the Late Quaternary: pollen evidence from Lake Masoko, Tanzania. *Journal of Biogeography* 34: 1274–1288.

Vincens, A., Lézine, A., Buchet, G., Lewden, D. & Le Thomas, A. 2007b. African pollen database inventory of tree and shrub pollen types. *Review of Palaeobotany and Palynology* 145: 135–141.

Wald, A. 1940. The fitting of straight lines if both variables are subject to error. *The Annals of Mathematical Statistics* 11: 284–300.

White, F. 1983. *The vegetation of Africa, a descriptive memoir to accompany the UNESCO/AETFAT/UNSO vegetation map of Africa*. UNESCO, Paris, FR.

Williams, J. 2003. Variations in tree cover in North America since the last glacial maximum. *Global and Planetary Change* 35: 1–23.

Wirth, R., Weber, B. & Ryel, R.J. 2001. Spatial and temporal variability of canopy structure in a tropical moist forest. *Acta Oecologica* 22: 235–244.

Wright, H.E. Jr 1967. The use of surface samples in quaternary pollen analysis. *Review of Palaeobotany and Palynology* 2: 321–330.

Wynn, J. & Bird, M. 2007. C_4 derived soil organic carbon decomposes faster than its C_3 counterpart in mixed C_3/C_4 soils. *Global Change Biology* 13: 2206–2217.

Supporting Information

Additional supporting information may be found in the online version of this article:

Appendix S1. Confidence interval computation of *AP/NAP* and *D/P*.

Appendix S2. Derivation of LAI anomalies in palaeosequences.

Please note: Wiley-Blackwell are not responsible for the content or functionality of any supporting materials supplied by the authors. Any queries (other than missing material) should be directed to the corresponding author for the article.

Doi: 10.1111/j.1654-1103.2011.01335.x